

Electric modulation of the Fermi arc spin transport via three-terminal configuration in topological semimetal nanowires

Guang-Yu Zhu(祝光宇), Ji-Ai Ning(宁纪爱), Jian-Kun Wang(王建坤), Xin-Jie Liu(刘心洁), Jia-Jie Yang(杨佳洁), Ben-Chuan Lin(林本川), and Shuo Wang(王硕)
Citation: Chin. Phys. B, 2024, 33 (**1**): 017305. DOI: 10.1088/1674-1056/ace157
Journal homepage: http://cpb.iphy.ac.cn; http://iopscience.iop.org/cpb

What follows is a list of articles you may be interested in

Nonlinear current response and electric quantum oscillations in the Dirac semimetal Cd_3As_2

Hao-Nan Cui(崔浩楠), Ze-Nan Wu(吴泽南), Jian-Kun Wang(王建坤), Guang-Yu Zhu(祝光宇), Jia-Jie Yang(杨佳洁), Wen-Zhuang Zheng(郑文壮), Zhi-Min Liao(廖志敏), Shuo Wang(王硕), Ben-Chuan Lin(林本川), and Dapeng Yu(俞大鹏)
Chin. Phys. B, 2023, 32 (**8**): 087306. DOI: 10.1088/1674-1056/acd9c5

Negative magnetoresistance in Dirac semimetal Cd_3As_2 with in-plane magnetic field perpendicular to current

Hao-Nan Cui(崔浩楠), Guang-Yu Zhu(祝光宇), Jian-Kun Wang(王建坤), Jia-Jie Yang(杨佳洁), Wen-Zhuang Zheng(郑文壮), Ben-Chuan Lin(林本川), Zhi-Min Liao(廖志敏), Shuo Wang(王硕), and Da-Peng Yu(俞大鹏)
Chin. Phys. B, 2023, 32 (**7**): 077305. DOI: 10.1088/1674-1056/accd50

Generalization of the theory of three-dimensional quantum Hall effect of Fermi arcs in Weyl semimetal

Mingqi Chang(苌名起), Yunfeng Ge(葛云凤), and Li Sheng(盛利)
Chin. Phys. B, 2022, 31 (**5**): 057304. DOI: 10.1088/1674-1056/ac5c32

High-resolution angle-resolved photoemission study of large magnetoresistance topological semimetal $CaAl_4$

Xu-Chuan Wu(吴徐传), Shen Xu(徐升), Jian-Feng Zhang(张建丰), Huan Ma(马欢), Kai Liu(刘凯), Tian-Long Xia(夏天龙), and Shan-Cai Wang(王善才)
Chin. Phys. B, 2021, 30 (**9**): 097303. DOI: 10.1088/1674-1056/ac0cd7

Topological transport in Dirac electronic systems: A concise review

Hua-Ding Song(宋化鼎), Dian Sheng(盛典), An-Qi Wang(王安琦), Jin-Guang Li(李金光), Da-Peng Yu(俞大鹏), Zhi-Min Liao(廖志敏)
Chin. Phys. B, 2017, 26 (**3**): 037301. DOI: 10.1088/1674-1056/26/3/037301

Electric modulation of the Fermi arc spin transport via three-terminal configuration in topological semimetal nanowires

Guang-Yu Zhu(祝光宇)[1,2,†], Ji-Ai Ning(宁纪爱)[1,2,†], Jian-Kun Wang(王建坤)[1,2,†], Xin-Jie Liu(刘心洁)[1,2], Jia-Jie Yang(杨佳洁)[1,2], Ben-Chuan Lin(林本川)[1,2,3,‡], and Shuo Wang(王硕)[1,2,3,§]

[1] *Shenzhen Institute for Quantum Science and Engineering, Southern University of Science and Technology, Shenzhen* 518055, *China*
[2] *International Quantum Academy, Shenzhen* 518048, *China*
[3] *Guangdong Provincial Key Laboratory of Quantum Science and Engineering, Southern University of Science and Technology, Shenzhen* 518055, *China*

(Received 27 March 2023; revised manuscript received 4 June 2023; accepted manuscript online 25 June 2023)

Spin–momentum locking is a key feature of the topological surface state, which plays an important role in spintronics. The electrical detection of current-induced spin polarization protected by the spin–momentum locking in nonmagnetic systems provides a new platform for developing spintronics, while previous studies were mostly based on magnetic materials. In this study, the spin transport measurement of Dirac semimetal Cd_3As_2 was studied by three-terminal geometry, and a hysteresis loop signal with high resistance and low resistance state was observed. The hysteresis was reversed by reversing the current direction, which illustrates the spin–momentum locking feature of Cd_3As_2. Furthermore, we realized the on–off states of the spin signals through electric modulation of the Fermi arc via the three-terminal configuration, which enables the great potential of Cd_3As_2 in spin field-effect transistors.

Keywords: topological semimetal, spin–momentum locking, quantum transport, spin field-effect transistor

PACS: 73.20.–r, 73.20.At, 73.21.Hb, 75.47.–m **DOI:** 10.1088/1674-1056/ace157

Dirac semimetal has received great attention because of its unique quantum transport characteristics, such as higher carrier mobility,[1–4] negative magnetoresistance caused by chiral anomaly,[5–8] as well as extremely large magnetoresistance.[3,9,10] The Dirac semimetal can be transformed into the Weyl semimetal when the time-reversal symmetry is broken.[11] The surface dispersion relation of a Weyl semimetal is topologically equivalent to a non-compact Riemann surface without equal-energy contour that encloses the projection of the Weyl point,[11] leading to the emergence of Fermi arcs, which are a unique topological surface state.[12–17] Fermi arcs have been observed directly by angle-resolved photoemission spectroscopy, which has the characteristic of spin–momentum locking.[18,19]

Spin-momentum locking means the spin of the electrons is locked perpendicular to the carrier's momentum, as shown in Fig. 1(a). This is caused by a strong spin–orbit interaction, which has been observed earlier in the three-dimensional topological insulators,[20,21] as well as the topological Dirac/Weyl semimetals,[18,22–24] through optical and transport measurements. Given that current can induce spin polarization protected by the spin–momentum locking, the electrical detection and control of this key feature are valuable for its application in energy-efficient spintronic devices.[22,25–27] However, previous studies of the spin–momentum locking property in topological materials including topological insulators mostly reported the electric current control of the spin signal, while few reported the electric gate control of the spin signal. Gate control is important because the probable spintronics application would be much more promising if the spin signal can be turned on/off (e.g., a novel type of spin field-effect transistor could be realized).

In this work, spin transport measurements of Dirac semimetal Cd_3As_2 nanowires were carried out using a three-terminal configuration.[28] The resistance demonstrates that a hysteresis loop develops as the external magnetic fields sweep back and forth. A high (low) voltage state is demonstrated when the magnetization M of the ferromagnetic electrode (Co) is parallel (anti-parallel) to the spin polarization s of the carriers. This hysteresis resistance state can be reversed by altering the direction of the current, revealing the spin–momentum locking feature of the Cd_3As_2 nanowires. Furthermore, the spin signal can be tuned by the gate voltage, which enables the spin transport on–off states.

The Cd_3As_2 nanowires grown by chemical vapor deposition (CVD) have high quality, large surface volume ratio, and low carrier density.[24,29] Three-terminal geometry measurements were applied for the electrical detection of the spin transport of Cd_3As_2 nanowires. A schematic of the device is displayed in Fig. 1(b), in which the ferromagnetic electrode (Co), indicated by blue, is located between the two outer nonmagnetic electrodes (Au), indicated by yellow. The left Au

[†]These authors contributed equally to this work.
[‡]Corresponding author. E-mail: linbc@sustech.edu.cn
[§]Corresponding author. E-mail: wangs6@sustech.edu.cn

© 2024 Chinese Physical Society and IOP Publishing Ltd

electrode and the middle Co electrode were used to apply current, while the right Au electrode and the middle Co were used to measure the spin signal. The three-terminal geometry was used to separate the current and the voltage circuits, which can limit the anisotropic magnetoresistance[30] and anomalous Hall effect induced by the Co electrodes.[31] An external in-plane magnetic field B parallel to the long axis of the Co electrode was applied to control the magnetization of the Co electrode. The direction along $+y$ is defined as positive B, while the current along $+x$ is defined as positive. The contacts were patterned via electron beam lithography and were deposited sequentially by electron beam evaporation (EBE). A scanning electron microscopy (SEM) image of the fabricated device is shown in Fig. 1(c), in which the Cd_3As_2 nanowire has a diameter of about 150 nm and the width of the ferromagnetic electrode (Co) is 500 nm, while the width of the Au electrodes is 1 μm.

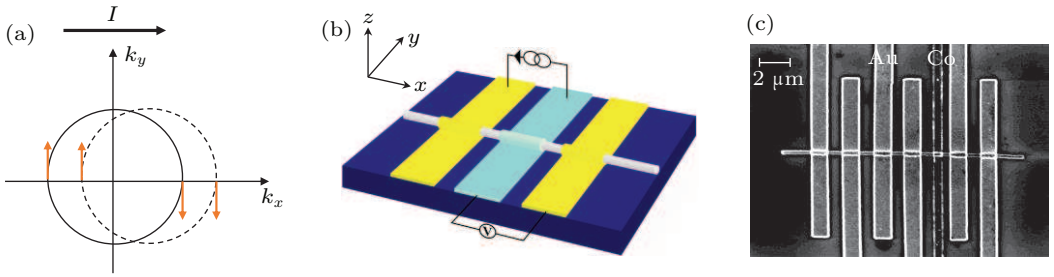


Fig. 1. (a) Schematic illustrations of the k_x–k_y plane of the surface states. Spin is locked to the momentum at each point. (b) The three-terminal geometry measurement diagram, which is used to separate the current and voltage circuits. The middle is a Co electrode indicated by blue and the two outer electrodes are Au electrodes indicated by yellow. (c) The scanning electron microscope image of a typical device.

The three-terminal geometry measurement under $T = 2$ K was carried out and the results are shown in Fig. 2. In which a high voltage state and a low voltage state displayed as a hysteresis loop were observed as the external in-plane magnetic field was sweeping back and forth. When $I_{dc} = 100$ nA, the momentum carries along the $-x$ direction (indicated by the black arrow). Due to the spin–momentum locking, the left-moving electrons have a spin-up polarization s pointing along the $+y$ direction (indicated by the red arrow), as shown in Fig. 2(a). When the magnetization of the Co electrode is $+M$ (indicated by the blue arrow) under a positive field, the relative orientation between electron spin s and $+M$ is parallel, which leads to a high resistance state. When the field swept from a positive to a negative field, the magnetization of the Co electrode is $-M$, and therefore electron spin s is anti-parallel to the $-M$ and a low resistance state was formed.

When the current direction was reversed, i.e., $I = -100$ nA, the spin polarization of electrons s is also reversed due to the spin–momentum locking (indicated by the red arrow) as shown in Fig. 2(b). Therefore, the relative orientation between s and $+M$ is anti-parallel under a positive and parallel under a negative field, respectively. As a result, a reversed hysteresis loop signal can be formed, as shown in Fig. 2(b). The reversed current leading to the reversed hysteresis loop unambiguously reveals the spin–momentum-locking properties of Cd_3As_2 nanowires.

Furthermore, gate voltage V_g tunable measurements[32] were carried out, and the results are shown in Fig. 3(a). Here the back gate was applied to the silicon wafer substrate with 285 nm silicon oxide as the dielectric layer. When the applied gate voltage is in the range from -4 V to $+4$ V, an obvious hysteresis loop signal can be observed. As the voltage increases, the hysteresis loop signal is weakened. When the voltage reached ± 6 V, the hysteresis loops are vague. Eventually, the spin signals disappeared at a negative voltage of -8 V and a positive $+10$ V, respectively.

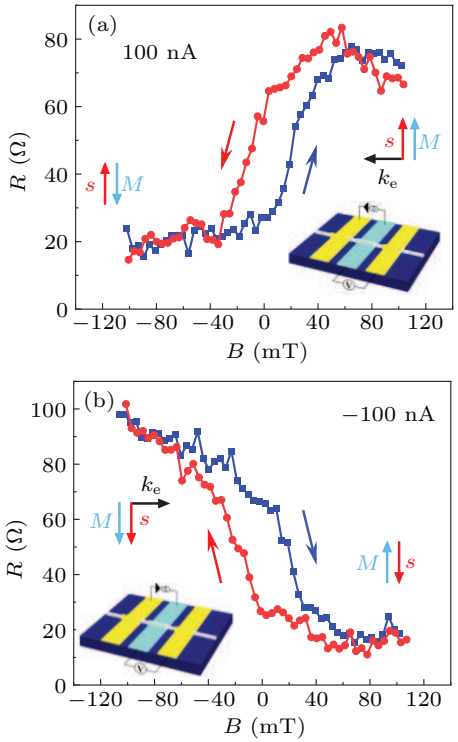


Fig. 2. Three-terminal measurement at 2 K. (a) A hysteretic loop signal measured under $I_{dc} = 100$ nA. (b) A hysteretic loop signal measured under $I_{dc} = -100$ nA. The high resistance states and low resistance states are reversed as the current direction is reversed, showing the spin–momentum locking feature.

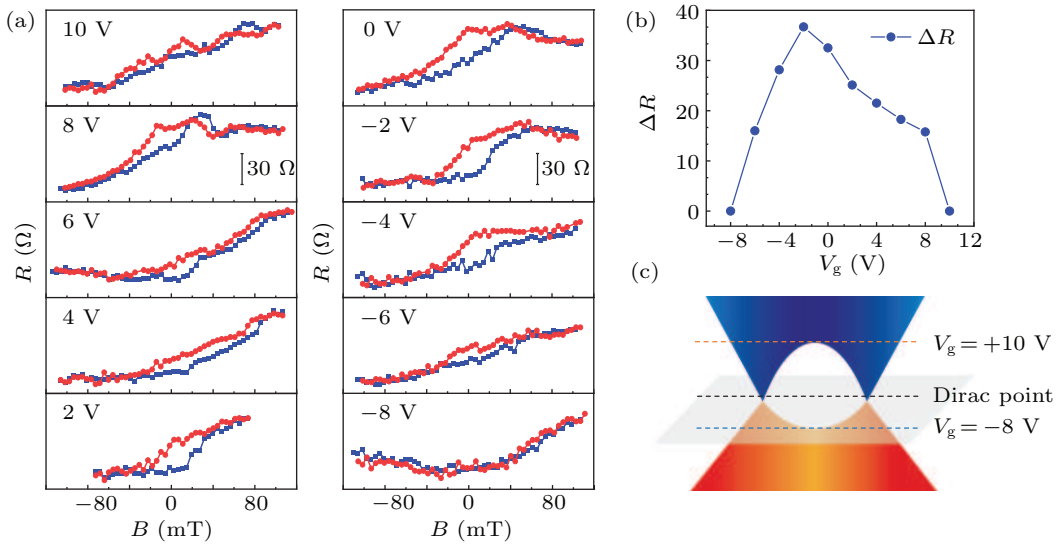


Fig. 3. (a) The hysteretic loop signals under various gate voltages. (b) The gate voltage V_g dependence of the height between the high resistance state and the low resistance state. (c) Schematic diagram of the spin signal on–off state under various gate voltages.

To illustrate the gate dependence of the spin signals, we define the height between the high resistance and the low resistance states as ΔR. The extracted ΔR from Fig. 3(a) as a function of the gate voltage is shown in Fig. 3(b). The values of ΔR display a peak at $V_g = -2$ V. As the absolute value of gate voltage increases, the ΔR decreases. The spin signals are significantly tuned by the gate voltage. Moreover, on–off states can be realized by modulating the gate voltage. The complete on–off spin transport states tuned by the gate voltage enable Cd_3As_2 have great potential in the spin field-effect transistor. The mechanism of the spin signal tuned by gate voltages can be understood as follows. When the Fermi level is close to the Dirac point $V_g = -2$ V, as shown in Fig. 3(c), the spin signal contributed by the Fermi arc reaches its maximum value. When the Fermi level is far from the Dirac point, the contributions from the Fermi arc are weakened, which results in a decrease in the spin signals. When the applied V_g is larger than 10 V or V_g is less than -8 V, the spin signals disappear completely. The reason for the complete disappearance of the signal may be attributed to the appearance of a topological phase transition, which is likely to come from the Lifshitz transition.[9–15,17,24]

In summary, we observed a hysteresis loop signal with high resistance and low resistance state through three-terminal geometry measurements, which reveal current-induced spin polarization in the surface state of Dirac semimetals Cd_3As_2 nanowires. Compared to traditional four-terminal configuration, the three-terminal configuration could have a considerably smaller device size in future spintronics applications. The high resistance and low resistance state are reversed while reversing the current direction, which illustrates the spin–momentum locking feature of Cd_3As_2 nanowires. Furthermore, the on–off control of the spin signal can be realized by tuning the gate voltage, which enables the great potential of Cd_3As_2 nanowires in the spin field-effect transistor. Our results provide a new perspective for future spintronic devices.

Acknowledgements

Project supported by the National Key Research and Development Program of China (Grant Nos. 2020YFA0309300 and 2022YFA1403700), the National Natural Science Foundation of China (Grant Nos. 12004158, 12074162, and 91964201), the Key-Area Research and Development Program of Guangdong Province (Grant No. 2018B030327001), Guangdong Provincial Key Laboratory (Grant No. 2019B121203002), and Guangdong Basic and Applied Basic Research Foundation (Grant No. 2022B1515130005).

References

[1] Liang T, Gibson Q, Ali M N, Liu M, Cava R J and Ong N P 2015 *Nat. Mater.* **14** 280
[2] Lv B Q, Qian T and Ding H 2021 *Rev. Mod. Phys.* **93** 025002
[3] Shekhar C, Nayak A K, Sun Y, Schmidt M, Nicklas M, Leermakers I, Zeitler U, Skourski Y, Wosnitza J, Liu Z, Chen Y, Schnelle W, Borrmann H, Grin Y, Felser C and Yan B 2015 *Nat. Phys.* **11** 645
[4] Zhao Y, Liu H, Zhang C, Wang H, Wang J, Lin Z, Xing Y, Lu H, Liu J, Wang Y, Brombosz S M, Xiao Z, Jia S, Xie X C and Wang J 2015 *Phys. Rev. X* **5** 031037
[5] Li C Z, Wang L X, Liu H, Wang J, Liao Z M and Yu D P 2015 *Nat. Commun.* **6** 10137
[6] Li H, He H, Lu H Z, Zhang H, Liu H, Ma R, Fan Z, Shen S Q and Wang J 2016 *Nat. Commun.* **7** 10301
[7] Jia Z, Li C, Li X, Shi J, Liao Z, Yu D and Wu X 2016 *Nat. Commun.* **7** 13013
[8] Xiong J, Kushwaha S K, Liang T, Krizan J W, Hirschberger M, Wang W, Cava R J and Ong N P 2015 *Science* **350** 413
[9] Cai P L, Hu J, He L P, Pan J, Hong X C, Zhang Z, Zhang J, Wei J, Mao Z Q and Li S Y 2015 *Phys. Rev. Lett.* **115** 057202
[10] Kumar N, Sun Y, Xu N, Manna K, Yao M, Suss V, Leermakers I, Young O, Forster T, Schmidt M, Borrmann H, Yan B, Zeitler U, Shi M, Felser C and Shekhar C 2017 *Nat. Commun.* **8** 1642
[11] Soluyanov A A, Gresch D, Wang Z, Wu Q, Troyer M, Dai X and Bernevig B A 2015 *Nature* **527** 495

[12] Fang C, Lu L, Liu J and Fu L 2016 *Nat. Phys.* **12** 936

[13] Wan X, Turner A M, Vishwanath A and Savrasov S Y 2011 *Phys. Rev. B* **83** 205101

[14] Armitage N P, Mele E J and Vishwanath A 2018 *Rev. Mod. Phys.* **90** 015001

[15] Moll P J, Nair N L, Helm T, Potter A C, Kimchi I, Vishwanath A and Analytis J G 2016 *Nature* **535** 266

[16] Potter A C, Kimchi I and Vishwanath A 2014 *Nat. Commun.* **5** 5161

[17] Li P, Wen Y, He X, Zhang Q, Xia C, Yu Z M, Yang S A, Zhu Z, Alshareef H N and Zhang X X 2017 *Nat. Commun.* **8** 2150

[18] Xu S Y, Liu C, Kushwaha S K, Sankar R, Krizan J W, Belopolski I, Neupane M, Bian G, Alidoust N, Chang T R, Jeng H T, Huang C Y, Tsai W F, Lin H, Shibayev P P, Chou F C, Cava R J and Hasan M Z 2015 *Science* **347** 294

[19] Xu S Y, Belopolski I, Alidoust N, Neupane M, Bian G, Zhang C, Sankar R, Chang G, Yuan Z, Lee C C, Huang S M, Zheng H, Ma J, Sanchez D S, Wang B, Bansil A, Chou F, Shibayev P P, Lin H, Jia S and Hasan M Z 2015 *Science* **349** 613

[20] Li C H, Erve O M J, Robinson J T, Liu Y, Li L and Jonker B T 2014 *Nat. Nanotechnol.* **9** 218

[21] Tang J, Chang L T, Kou X, Murata K, Choi E S, Lang M, Fan Y, Jiang Y, Montazeri M, Jiang W, Wang Y, He L and Wang K L 2014 *Nano Lett.* **14** 5423

[22] Li P, Wu W, Wen Y, Zhang C, Zhang J, Zhang S, Yu Z, Yang S A, Manchon A and Zhang X X 2018 *Nat. Commun.* **9** 3990

[23] Ning J, Peng W, Wang W, Chen Z, Yang P, Chen Y, Zhao Y, Sun Y, Kanagaraj M, Yang L, Gao Q, Zhang J, Zhao D, Pan D, Ruan X, Li Y, Liu W, He L, Chen Z G and Xu Y 2021 *Phys. Rev. B* **104** 035429

[24] Lin B C, Wang S, Wang A Q, Li Y, Li R R, Xia K, Yu D and Liao Z M 2020 *Phys. Rev. Lett.* **124** 116802

[25] Han J, Richardella A, Siddiqui S A, Finley J, Samarth N and Liu L 2017 *Phys. Rev. Lett.* **119** 077702

[26] Wang Y, Zhu D, Wu Y, Yang Y, Yu J, Ramaswamy R, Mishra R, Shi S, Elyasi M, Teo K L, Wu Y and Yang H 2017 *Nat. Commun.* **8** 1364

[27] Yasuda K, Tsukazaki A, Yoshimi R, Kondou K, Takahashi K S, Otani Y, Kawasaki M and Tokura Y 2017 *Phys. Rev. Lett.* **119** 137204

[28] Ando Y, Hamasaki T, Kurokawa T, Ichiba K, Yang F, Novak M, Sasaki S, Segawa K, Ando Y and Shiraishi M 2014 *Nano Lett.* **14** 6226

[29] Lin B C, Wang S, Wang L X, Li C Z, Li J G, Yu D, Liao Z M 2017 *Phys. Rev. B* **95** 235436

[30] Tang J, Wang C Y, Chang L T, Fan Y, Nie T, Chan M, Jiang W, Chen Y T, Yang H J, Tuan H Y, Chen L J and Wang K L 2013 *Nano Lett.* **13** 4036

[31] Nagaosa N, Sinova J, Onoda S, MacDonald A H and Ong N P 2010 *Rev. Mod. Phys.* **82** 1539

[32] Wang H L, Ma J L and Wei Q Q 2020 *J. Semicond.* **41** 072903